JOURNAL OF VIROLOGY, June 2004, p. 5564–5575 Vol. 78, No. 11
0022-538X/04/$08.00+0 DOI: 10.1128/JVI.78.11.5564–5575.2004

Conformational Changes in the Nuclear Lamina Induced by Herpes Simplex Virus Type 1 Require Genes U_L31 and U_L34

Ashley E. Reynolds,†‡ Li Liang,† and Joel D. Baines*

Department of Microbiology and Immunology, Cornell University, Ithaca, New York 14853

Received 18 November 2003/Accepted 27 February 2004

The herpes simplex virus type 1 (HSV-1) U_L31 and U_L34 proteins are dependent on each other for proper targeting to the nuclear membrane and are required for efficient envelopment of nucleocapsids at the inner nuclear membrane. In this work, we show that whereas the solubility of lamins A and C (lamin A/C) was not markedly increased, HSV induced conformational changes in the nuclear lamina of infected cells, as viewed after staining with three different lamin A/C-specific antibodies. In one case, reactivity with a monoclonal antibody that recognizes an epitope in the lamin tail domain was greatly reduced in HSV-infected cells. This apparent HSV-induced epitope masking required both U_L31 and U_L34, but these proteins were not sufficient to mask the epitope in uninfected cells, indicating that other HSV proteins are also required. In the second case, staining with a rabbit polyclonal antibody that primarily recognizes epitopes in the lamin A/C rod domain revealed that U_L34 is required for HSV-induced decreased availability of epitopes for reaction with the antibody, whereas U_L31 protein was dispensable for this effect. Still another polyclonal antibody indicated virtually no difference in lamin A/C staining in infected versus uninfected cells, indicating that the HSV-induced changes are more conformational than the result of lamin depletion at the nuclear rim. Further evidence supporting an interaction between the nuclear lamina and the U_L31/U_L34 protein complex includes the observations that (i) overexpression of the U_L31 protein in uninfected cells was sufficient to relocalize lamin A/C from the nuclear rim into nucleoplasmic aggregates, (ii) overexpression of U_L34 was sufficient to relocalize some lamin A/C into the cytoplasm, and (iii) both U_L31 and U_L34 could directly bind lamin A/C in vitro. These studies suggest that the U_L31 and U_L34 proteins modify the conformation of the nuclear lamina in infected cells, possibly by direct interaction with lamin A/C, and that other proteins are also likely involved. Given that the nuclear lamina potentially excludes nucleocapsids from envelopment sites at the inner nuclear membrane, the lamina alteration may reflect a role of the U_L31/U_L34 protein complex in perturbing the lamina to promote nucleocapsid egress from the nucleus. Alternatively, the data are compatible with a role of the lamina in targeting the U_L31/U_L34 protein complex to the nuclear membrane.

The nuclear envelope consists of two leaflets, defined as the inner nuclear membrane and outer nuclear membrane. The perinuclear space, defined as the space between the two leaflets, is continuous with the lumen of the endoplasmic reticulum. A network of predominantly insoluble cellular proteins, the nuclear lamina, lines the nucleoplasmic face of the inner nuclear membrane. The nuclear lamina provides structural support for the nuclear membrane and attachment sites for chromatin. It is also required for a variety of essential cellular functions, including nuclear assembly following mitosis, DNA replication, and transcription (11, 29).

The nuclear lamina is composed primarily of type V intermediate filament proteins known as lamins. Lamin structure is conserved in multicellular eukaryotes, and individual lamin filaments consist of multiple coiled-coil dimers linked in a head-to-tail fashion. Lamin filaments are nucleoskeletal components in interphase cells and therefore normally remain insoluble under a variety of extraction conditions. Differentiated mammalian cells express two types of lamins. A-type lamins include lamin A (the full-length product of the *Lmna* gene) and a smaller RNA splice variant termed lamin C (7, 18, 19). In somatic cells, the second lamin type includes lamins B1 and B2, which are encoded by genes distinct from *Lmna* (12, 14). Consistent with the canonical structure of cytoplasmic intermediate filaments, A- and B-type lamins consist of a head domain, a central rod domain of about 350 amino acids containing heptad repeats, a tail domain, and a CaaX (where a is an aliphatic amino acid and X is any amino acid) isoprenylation motif at the carboxyl terminus. The final 90 amino acids of lamin A are replaced with six unique amino acids of lamin C and lack the isoprenylation motif.

A remarkable feature of the nuclear lamina is its disassembly during mitosis and reassembly following metaphase. Although the precise mechanism of the breakdown of the nuclear lamina has not been fully delineated, it is known that mitosis-promoting factor kinase $p34^{cdc2}$ phosphorylates a number of envelope-associated proteins, resulting in disruption of lamin-lamin interactions that are essential for the integrity of the nuclear envelope. Dephosphorylation of lamins is associated with reformation of the lamin filament network following mitosis (10).

Herpes simplex virus type 1 (HSV-1), like all herpesviruses, assembles nucleocapsids containing DNA within the nuclei of infected cells. The nucleocapsids bud from sites within the inner nuclear membrane to become enveloped viral particles in

* Corresponding author. Mailing address: Dept. of Microbiology and Immunology, VMC C5 131, Cornell University, Ithaca, NY 14853. Phone: (607) 253-3385. Fax: (607) 253-3384. E-mail: jdb11@cornell.edu.

† A.E.R. and L.L. contributed equally to this work.

‡ Present address: Deptartment of Molecular Biology, Princeton University, Princeton, NJ 08544.

TABLE 1. Primer pairs used to generate lamin A subclones

Primer pair	Lamin A codons	Name of encoded protein	Plasmid
GCCGCCATGGAGACCCCGTCCCAGCGG and TCATTACAGCCGAGCCTGAGCAGCT	1–129	GST/Head	pJB326
GCCGCCATGGCGCGCAATACCAAGAAGGA and TCAGTCAGTCACGCTCTCAAACTCACGCTGCT	117–239	GST/Rod1	pJB327
GCCGCCATGGAGACCAAGCGCCGTCATGA and TCAGTCAGTCACCAGGCGTAGCCTCTCCTCCT	216–384	GST/Rod2	pJB328
TCCGACATGGAGATCCACGCCTA and TCAGTCAGTCACGGTGTTCTGTGCCTTCCACA	369–519	GST/Tail1	pJB329
GCCGCCATGGGGCAGGTGGTGACGATCT and TCAGTCAGTCACGTTCTGGGGGCTCTGGGTT	490–660	GST/Tail2	pJB330

a process termed primary envelopment. Inasmuch as the insoluble lamina underlying the inner nuclear membrane would be expected to present a barrier to herpesvirus envelopment, it is logical that herpesviruses would modify the nuclear lamina to allow access to primary envelopment sites at the inner nuclear membrane. For example, murine cytomegalovirus (MCMV), a betaherpesvirus, encodes M50/p35, an integral membrane protein, and its MCMV-encoded binding partner M50/p38. Complexes of these proteins recruit protein kinase C to the nuclear lamina to phosphorylate and likely disassemble the nuclear lamina (20). Thus, a mechanism similar to the endogenous mechanism for breakdown of the nuclear lamina during mitosis may have been co-opted by MCMV to allow primary envelopment of viral particles. A protein encoded by equine herpesvirus, IR6, has also been shown to associate with the nuclear lamina and under some conditions promotes egress of nucleocapsids from the nucleus (21).

It has been suggested that HSV-1 utilizes a mechanism similar to that of MCMV, wherein lamins are altered by phosphorylation to ultimately allow egress of nucleocapsids from the nucleus, but others have not detected a difference in phosphorylation of lamins in HSV-infected cells (23, 27).

HSV-1 U_L31 protein is a homolog of MCMV M50/p38 and is a nuclear matrix-associated phosphoprotein stabilized by its interaction with an integral membrane protein of HSV-1 encoded by U_L34 (the homolog of MCMV M50/p35) (3, 33). The two HSV proteins interact to form a complex targeted to both leaflets of the nuclear membrane, and similar studies have shown that this is also true for pseudorabies virus of swine (9, 24, 25, 32, 34). The U_L31 and U_L34 proteins are individually required for primary envelopment of nucleocapsids and proper targeting of the complex to the nuclear membrane (25, 26, 32). Based on the data presented herein, we propose that HSV mediates a restructuring of the nuclear lamina and that this restructuring is mediated, at least in part, by physical interaction between the HSV-1 U_L31/U_L34 protein complex and lamin A/C.

MATERIALS AND METHODS

Cells and viruses. Wild-type HSV-1(F), the U_L31 and U_L34 deletion viruses, and viruses derived from these bearing restored U_L31 and U_L34 genes have been described previously (4, 6, 26).

Plasmids. A full-length lamin A cDNA construct (kindly provided by David Gilbert, Upstate Medical Center, State University of New York) was amplified by PCR with an upstream primer (5′-CCC*GGATCC*ATGGAGACCCCGTCC CAG) containing a BamHI site, whereas the downstream primer (5′ TTG*CTC GAG*TCATGATGCTGCAGTTCTG) was engineered to contain an XhoI site (restriction sites are in italics). The PCR product was cloned as a BamHI/XhoI fragment into the vector pGEX4T-1 so that the full-length lamin A gene was cloned in frame with the gene encoding glutathione *S*-transferase (GST). All other lamin A constructs were generated by PCR with the primers shown in Table 1, and the amplicons were cloned into a T/A cloning vector (pCR3.1; Invitrogen). Lamin A sequences were subsequently released by EcoRI digestion and cloned into the EcoRI site of pGEX 2T in frame with the gene encoding GST. The designations of the plasmids and their encoded proteins are indicated in Table 1.

The plasmid encoding full-length lamin A-GST was designated pJB311; a plasmid encoding lamin A amino acids 1 to 129 fused to GST was designated pJB326 and the encoded protein was designated GST/Head; plasmid pJB327 contains lamin A amino acids 117 to 239 fused to GST, and the protein expressed from this construct was named GST/Rod1; a plasmid designated pJB328 contains lamin A amino acids 216 to 384 and encoded the protein GST/Rod2. Lamin A amino acids 369 to 519 fused to GST are carried by plasmid pJB329 and encode GST/Tail1; the protein GST/Tail2 is encoded by plasmid pJB330, containing the coding sequence for lamin A amino acids 490 to 660 fused to GST. DNA at the lamin A-GST junctions of the various fusion proteins was sequenced to ensure that the open reading frames were maintained.

Expression and purification of lamin-GST fusion proteins. The constructs described above were used to chemically transform *Escherichia coli* BL21(DE3) codon plus bacteria for expression of protein. For production of lamin A-GST, 10 ml of fresh stationary-phase culture was inoculated into 1 liter of Luria broth (LB) supplemented with ampicillin. To optimize expression and minimize degradation, the bacterial culture was grown at 30°C until the optical density at 595 nm was 0.5, at which time protein expression was induced by the addition of 0.5 mM isopropylthiogalactopyranoside (IPTG). The culture was shaken at 210 rpm at 28°C for 2 h in a 2-liter Erlenmeyer flask. Bacteria were pelleted and lysed as described by Frangioni and Neel (8), except that (i) one tablet of complete EDTA-free protease inhibitor cocktail (Roche; effective for 50 ml of cell culture) was added during bacterial lysis with lysozyme and Sarkosyl and (ii) the bacterial mixture was lysed with approximately 30 strokes with a Dounce homogenizer until the mixture was clear, with minimal foaming. The final supernatant contained 1.5% Sarkosyl and 4% Triton X-100 in cold STE buffer (Tris-HCl [pH 8.0], 1 mM EDTA, 150 mM NaCl). This mixture was incubated at 4°C overnight with glutathione Sepharose 4B beads (Amersham Biosciences). The beads were then pelleted and washed extensively with cold sterile phosphate-buffered saline (PBS). The final mixture was placed in storage buffer (50 mM HEPES buffer [pH 7.4], 150 mM NaCl, 5 mM dithiothreitol, 10% [vol/vol] glycerol) and maintained at 4°C for further experimental use.

Lamin epitope mapping. The BL21(DE3) codon plus strain of *E. coli* (Stratagene) was chemically transformed with the various plasmids encoding full-length and truncated lamin A sequences fused to GST, and 5 ml of overnight cultures was added to 100-ml aliquots of LB supplemented with ampicillin and 0.5 mM IPTG. After 3 h of vigorous shaking at 30°C, the bacteria in the cultures

were pelleted, and the bacterial fusion proteins were purified by affinity chromatography on glutathione-conjugated Sepharose 4B beads as described above. Approximately 1 μg of each fusion protein, as determined by comparison to known protein standards, was electrophoretically separated on a denaturing polyacrylamide gel and transferred to nitrocellulose. The nitrocellulose sheet was probed with a 1:200 dilution of a commercial immunoglobulin G2b monoclonal antibody specific for lamin A/C (Santa Cruz Biotechnology; catalog number sc-7292) or with a 1:500 dilution of rabbit polyclonal anti-lamin serum (Cell Signaling Technologies). Bound immunoglobulin was revealed with an alkaline phosphatase-conjugated donkey anti-mouse immunoglobulin antibody or alkaline phosphatase-conjugated donkey anti-rabbit immunoglobulin antibody as previously described (1).

Indirect immunofluorescence assays of infected cells. HEp-2 cells were seeded at 80% confluency and allowed to adhere to the bottom of the flask 8 or more h before infection. The cells were either mock infected or infected with wild-type HSV-1(F), the U_L31 null mutant virus, U_L34 mutant deletion virus, or a virus derived from the U_L34 deletion virus but bearing a restored U_L34 gene (26) at a multiplicity of infection (MOI) of 5 PFU/cell. At 16 h postinfection, cells were fixed and permeabilized in ice-cold methanol as described previously (24). Cells were then blocked with excess human serum and probed with ICP8 polyclonal antiserum (courtesy of W. Ruyechan, State University of New York at Buffalo) prepared as described previously (24) and with the lamin A/C-specific mouse monoclonal ascites fluid (Santa Cruz Biotechnology). Bound antibodies were visualized with Texas Red-conjugated donkey anti-rabbit immunoglobulin antibodies and fluorescein isothiocyanate (FITC)-conjugated donkey anti-mouse immunoglobulin antibodies.

In some experiments, rabbit polyclonal lamin antiserum (Cell Signaling Technologies/New England Biotech) was used to stain cells that were costained with monoclonal ICP4 antibodies (Goodwin Institute for Cancer Research). In these cases, bound lamin antibodies were detected with Alexa 488 fluorophore-conjugated secondary antibodies (Molecular Probes), and antibody bound to ICP4 was detected with Alexa 568 fluorophore-conjugated antibodies (Molecular Probes).

In all experiments, stained cells were visualized with a 63× oil objective mounted on an Olympus confocal microscope. Digital images were captured with Fluoview software, and formatting of the images was performed with Adobe Photoshop version 6.0 software.

Extraction and quantification of soluble lamins in cells by immunoblot analysis. To quantify the levels of soluble and insoluble lamin A/C, monolayers of HEp-2 cells were mock infected or infected with wild-type HSV-1(F) at an MOI of 5 PFU/cell. At 16 h postinfection, the monolayer in each flask was washed three times with cold sterile PBS, and the cells were scraped from the flask and pelleted by centrifugation. The pellets were resuspended in equal amounts of cold sterile PBS, and the total protein level per 100 μl of resuspended cells was determined by a modified Bradford assay (Bio-Rad). Cells corresponding to 200 μg of total protein were vigorously pipetted to ensure complete suspension in extraction buffer and extracted for 2 min on ice in a volume equal to that of the cell pellet in buffer containing 0.5% NP-40, 10 mM HEPES-KOH (pH 7.9), 1.5 mM $MgCl_2$, 10 mM KCl, 0.5 mM dithiothreitol, and complete protease inhibitor (Roche). The buffers were supplemented with either 0 mM NaCl, 500 mM NaCl, or 2 M NaCl. The soluble and insoluble fractions were separated by centrifugation at 12,000 × *g* at room temperature for 15 min and resuspended in 2× sodium dodecyl sulfate-polyacrylamide gel electrophoresis (SDS-PAGE) loading buffer containing 20% glycerol, 5% SDS, bromophenol blue, 10 mM β-mercaptoethanol, and 10 mM Tris-HCl, pH 8.0.

To facilitate loading of the pelleted material into the wells of the acrylamide gel, the insoluble fraction was briefly sonicated in the 2× loading buffer. After resuspension in SDS-PAGE buffer, all samples were boiled for 5 min, electrophoretically resolved on an SDS–8% polyacrylamide gel, and then electrically transferred from the gel onto a nitrocellulose membrane. The nitrocellulose was blocked for 1 h at room temperature in a 5% (wt/vol) nonfat dry milk–1% (vol/vol) Tween 20 solution of PBS. The blocked membrane was probed with lamin A/C-specific monoclonal antibody and then incubated with goat anti-mouse alkaline phosphatase-conjugated secondary antibody for 1 to 2 h and washed, and excessive moisture was removed. The nitrocellulose was incubated for 5 min with enhanced chemifluorescence (ECF) substrate (Amersham Biosciences), and the membrane was scanned in the blue channel of a Molecular Dynamics Storm 860 PhosphorImager. Chemiluminescent signals from the probed membrane were analyzed with ImageQuant software. The nitrocellulose membrane was then blocked overnight with the 5% milk–PBS blocking mixture and reprobed with adsorbed U_L31 polyclonal antiserum prepared as described previously (24). Bound U_L31 antiserum was detected by a goat anti-rabbit alkaline phosphatase-conjugated secondary antibody. The membrane was then incubated with a chromogenic substrate, 5-bromo-4-chloro-3-indolylphosphate (BCIP)/nitroblue tetrazolium (NBT) (Bio-Rad) in order to visualize U_L31 protein, and a digital representation of the U_L31 protein-specific band was generated by scanning the membrane with a Hewlett Packard tabletop scanner.

Analysis of transiently expressed U_L31 and U_L34 proteins in HEp-2 cells. HEp-2 cells were seeded on sterile coverslips at a density of approximately 30% and allowed to grow at 37°C to a density of approximately 50%. With Superfect transfection reagent (Qiagen), cells were transfected with 4.5 μg of pJB233, which is a full-length U_L31/pcDNA3 construct (24), 4.5 μg of pcDNA3 alone, 4.5 μg of pJB234 containing U_L34 driven by the cytomegalovirus immediate-early promoter/enhancer, or 2.5 μg of pJB233 together with 2.5 μg of pJB234. At 45 h posttransfection, cells were fixed in ice-cold methanol for 20 min at −20°C and rinsed thoroughly in PBS. The fixed cells were blocked with human serum as previously described (24) and incubated with U_L31 protein-specific rabbit polyclonal antiserum and lamin A/C monoclonal antibody. Bound primary antibodies were detected with donkey anti-rabbit immunoglobulin conjugated with Alexa 488 fluorophore and donkey anti-mouse immunoglobulin conjugated with Alexa 568 fluorophore. Fluorescence and Nomarski differential interference contrast digital micrographs were collected with Fluoview software with a 63× oil objective mounted on an Olympus confocal microscope.

In experiments analyzing U_L34 expression alone, transfected cells were fixed and blocked with 10% BlockHen II (Aves Lab, Inc.), stained with anti-U_L34 chicken antibody (1:4,000) and lamin A/C monoclonal antibody, and detected with Texas Red-conjugated donkey anti-chicken immunoglobulin and FITC-conjugated donkey anti-mouse immunoglobulin.

In cells cotransfected with U_L31 and U_L34, fixed cells were blocked with 10% human serum, stained with U_L31 rabbit antiserum and lamin A/C monoclonal antibody, blocked again with 10% BlockHen II, and reacted with the chicken antibody specific for U_L34 protein. Bound primary antibodies were detected with FITC-conjugated donkey anti-rabbit immunoglobulin, Texas Red-conjugated donkey anti-chicken immunoglobulin, and indodicarbocyanine-conjugated donkey anti-mouse immunoglobulin. Indodicarbocyanine staining was pseudocolored blue for illustrative purposes.

GST pulldown assays. U_L31-GST fusion protein was prepared as described previously (24). Full-length lamin A-GST was prepared as described above. Full-length lamin A was cloned into pSPORT1 so that transcription was under the control of the bacteriophage T7 promoter in the vector. Lamin A was expressed and radiolabeled with [^{35}S]methionine with this plasmid and a Promega TNT rabbit reticulocyte transcription-translation system in a total volume of 50 μl according to the directions of the manufacturer; 5 μl of the lamin protein reaction mixture was incubated overnight at 4°C with 20 μg of U_L31-GST fusion protein conjugated to Sepharose beads in cold PBS supplemented with 1% (vol/vol) Triton X-100 or 20 μg of GST. In the reciprocal reactions, [^{35}S]methionine-labeled U_L31 protein expressed in rabbit reticulocyte lysates was reacted with 20 μg of lamin A-GST fusion protein or 20 μg of GST. Following the incubation periods, the beads and bound proteins were washed four times with cold 1% Triton X-100. The washed beads with bound proteins were boiled in 2× SDS loading buffer and electrophoretically separated on an SDS–12% polyacrylamide gel. The gel was soaked for 30 min in 20% sodium salicylate and dried. Fluorography was performed with X-Omat (Kodak) film exposed overnight at −80°C.

Production, characterization, and immunostaining with anti-lamin A/C chicken antibody. Full-length lamin A/C fused to GST was purified by affinity chromatography as detailed above. The purified protein was denatured in SDS and electrophoretically separated on a denaturing polyacrylamide gel, and a single band revealed by brief staining with Coomassie blue was cut out of the gel, pulverized with a 21-gauge needle, and submitted for immunization to Aves Labs. Purified immunoglobulin Y from the yolks of chicken eggs obtained from birds before and after immunization was tested for reactivity to lamin A/C on immunoblots of lysates of infected and uninfected cells. The reactivity on immunoblots was identical to that of a commercially available rabbit polyclonal antibody that recognizes lamin A/C (data not shown).

HEp-2 cells were seeded on coverslips and mock infected or infected with wild-type HSV-1(F) virus, U_L31 deletion virus, U_L31 repair virus, U_L34 deletion virus, or U_L34 repair virus. Sixteen hours after infection, cells were fixed with ice-cold methanol for 20 min, immersed in 50 mM NH_4Cl for 15 min, and blocked with 10% human serum for 1 h. Cells were then washed three times with PBS supplemented with 0.2% Tween 20 for 5 to 15 min each time, stained with ICP4 monoclonal antibody at 1:1,000, and blocked again with 10% BlockHen II (Aves Labs)for 1 h. The cells were then washed in PBS plus 0.2% Tween 20 three times and stained with chicken anti-lamin antibody diluted 1:200 in PBS supplemented with 1% bovine serum albumin. Primary antibodies were recognized by FITC-conjugated donkey anti-chicken (Jackson ImmunoResearch) and Texas Red-conjugated donkey anti-mouse (Jackson ImmunoResearch) immunoglobu-

lins. Coverslips were placed on mounting reagent (Prolong anti-fade kit; Molecular Probes, Eugene, Oreg.) and examined as described above.

RESULTS

Effects of U_L31 and U_L34 on lamin A/C distribution in infected cells. To determine the fate of the nuclear lamina in HSV-infected cells, monolayers of HEp-2 cells were either mock infected or infected with wild-type virus HSV-1(F), a U_L31 null mutant virus, a virus lacking U_L34, or a virus derived from the U_L34 null virus but bearing a restored U_L34 gene. At 16 h postinfection, the cells were fixed and permeabilized at −20 C with ice-cold methanol. The cells were costained with lamin A/C monoclonal ascites fluid and a rabbit polyclonal antiserum recognizing ICP8, a marker for the replication compartments of infected cells, as described previously (16). Bound antibodies were visualized with Texas Red-conjugated donkey anti-rabbit antibodies and FITC-conjugated donkey anti-mouse antibodies. The stained cells were analyzed by confocal microscopy, and the images shown in Fig. 1 were acquired at identical settings. In mock-infected cells and cells infected with the U_L31 and U_L34 null mutant viruses, lamin A/C protein-specific staining was very similar and appeared to be evenly distributed around the nuclear rim. In contrast, the lamin staining appeared discontinuous along the nuclear rim of cells infected with wild-type HSV-1(F) or the virus bearing a restored U_L34 gene. Similar results were obtained with a virus bearing a restored U_L31 gene (not shown).

We reasoned that the discontinuous nature of the lamin staining in cells infected with wild-type HSV-1 might be caused by (i) degradation or displacement of lamin A/C from the nuclear rim or (ii) masking or alteration of the epitope recognized by the lamin-specific monoclonal antibody by direct or indirect interaction of the U_L31 or U_L34 protein with lamin A/C. To distinguish between these possibilities, cells were mock infected or infected with the U_L31 deletion virus, the U_L34 deletion virus, or a virus derived from the U_L34 deletion virus that contained a restored U_L34 gene. The cells were then costained with a lamin-specific rabbit polyclonal antisera and ICP4 monoclonal antibody as an infection marker (Fig. 2).

Lamin A/C distribution in mock-infected cells stained with the monoclonal antibody differed slightly from that in mock-infected cells stained with the polyclonal antibody, inasmuch as more nucleoplasmic lamin A/C was recognized. In addition, the appearance of mock-infected cells differed significantly from that of cells infected with HSV-1(F). In mock-infected cells, lamin A/C distribution localized in the nucleoplasm and nuclear rim, but in HSV-1(F)-infected cells, the intensity of lamin A/C staining was decreased considerably, to the point that the stain appeared almost exclusively at the nuclear rim. In contrast to the results obtained with the monoclonal antibody, anti-lamin A/C polyclonal antibody staining was distributed very similarly in cells infected with the U_L31 null virus or with HSV-1(F).

In contrast to the results with U_L31, the appearance of rabbit polyclonal anti-lamin A/C staining in cells infected with the U_L34 deletion virus was indistinguishable from that of mock-infected cells. That this effect was attributable to U_L34 was supported by the observation that the lamin A/C staining patterns of cells infected with the HSV-1(F) and U_L34 repair viruses were indistinguishable. Taken together, these data indicate that the U_L34 gene is required for decreased lamin A/C staining with both polyclonal and monoclonal antibodies, whereas only decreased monoclonal antibody staining is dependent on U_L31.

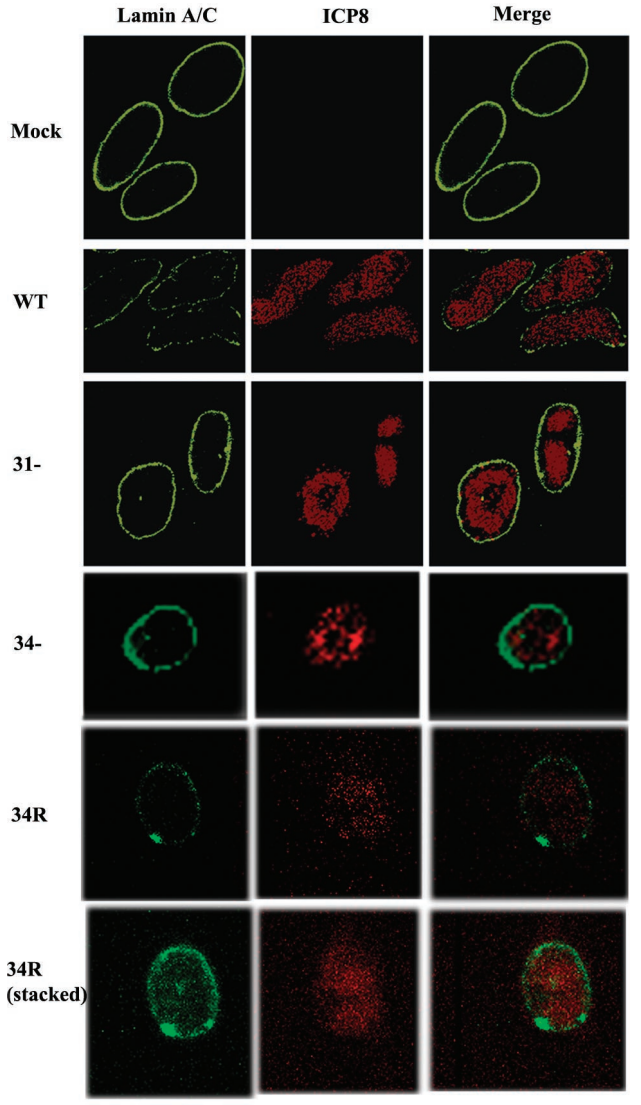

FIG. 1. Digital image of monoclonal antilamin A/C staining of HEp-2 cells that were mock infected, or infected with HSV-1(F) (WT), the U_L31 deletion virus (31−), U_L34 deletion virus (34−), or virus bearing a restored U_L34 gene (34R). Images were acquired at the same microscope settings. Cells were infected at an MOI of 5 and fixed and permeabilized in ice-cold methanol at 16 h postinfection (h.p.i.). Cells were blocked with 10% human serum in cold, sterile PBS supplemented with 1% bovine serum albumin and then incubated with rabbit polyclonal ICP8 antiserum, as an HSV infection marker, and lamin A/C monoclonal antibody. Bound antibodies were visualized with Texas Red-conjugated donkey anti-rabbit antibodies (red, ICP8 staining) and FITC-conjugated donkey anti-mouse antibodies (green, lamin A/C staining). The cells were analyzed with an Olympus confocal microscope with a 63× oil objective. Digital images from a single focal plane were acquired with Fluoview software. In the bottom row, a superimposed image of the optical sections of the cell shown in row 34R is shown to better illustrate the ICP8 staining.

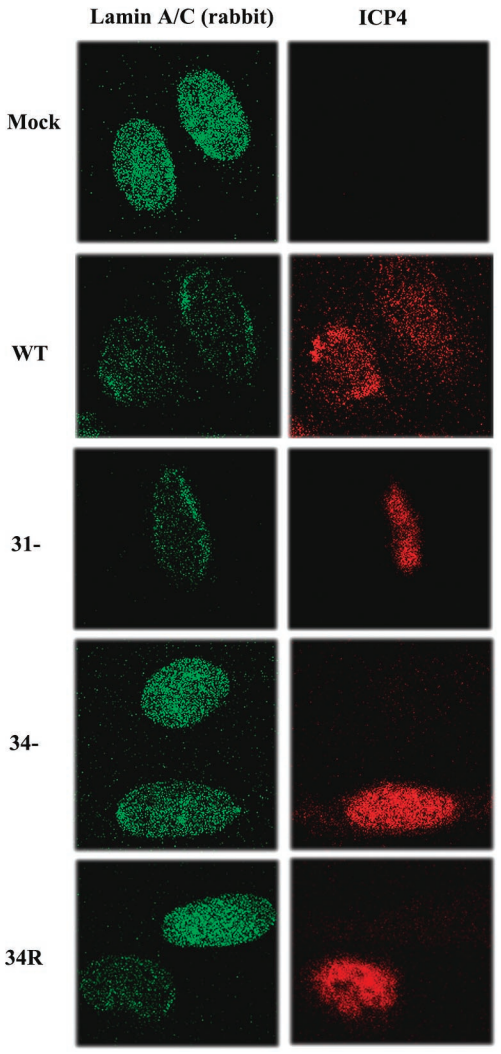

FIG. 2. Digital images of rabbit polyclonal antilamin A/C staining of HEp-2 cells that were mock infected or infected with HSV-1(F) (WT), U_L31 null mutant (31−), U_L34 null mutant (34−), or a virus bearing a restored U_L34 gene (34R). Cells were infected at an MOI of 5. At 16 h postinfection (h.p.i.), cells were fixed and permeabilized with ice-cold methanol and incubated with rabbit polyclonal antiserum recognizing lamin A/C and ICP4 monoclonal antibody to mark infected cells. Bound antibodies were detected with Alexa 488 fluorophore-conjugated goat anti-rabbit antibody (yielding a green signal for positive lamin staining) and Alexa 568 fluorophore-conjugated goat anti-mouse secondary antibody (yielding a red signal for positive ICP4 staining).

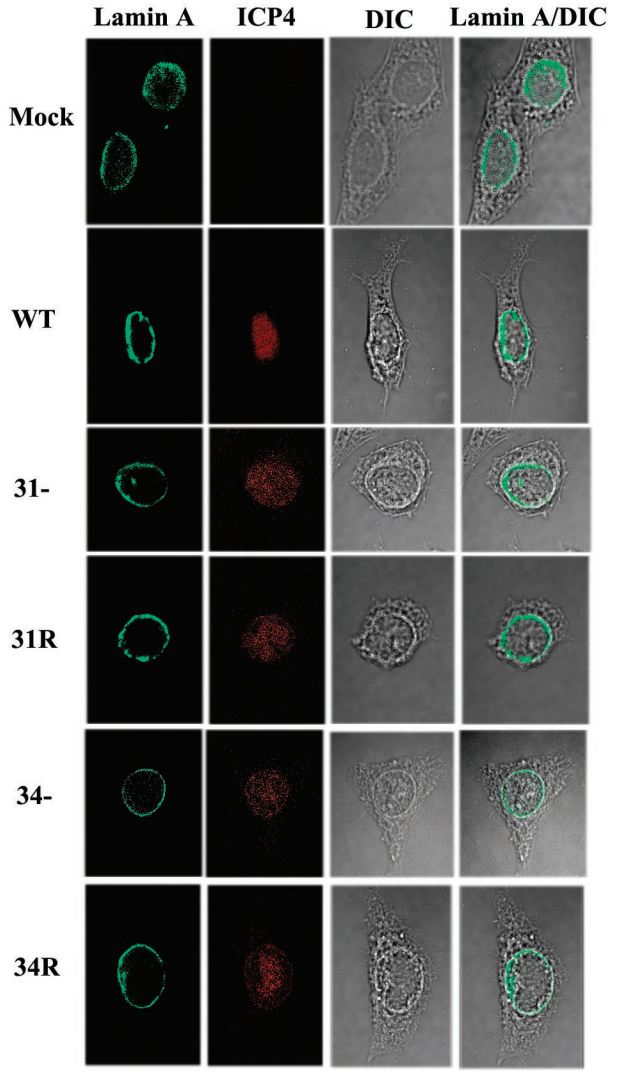

FIG. 3. Digital images of mock-infected cells and infected cells stained with chicken polyclonal immunoglobulin Y directed against lamin A/C. Cells were mock infected or infected with HV-1(F) (WT), the U_L31 and U_L34 deletion viruses (31− and 34−, respectively), or viruses derived from these two that bore restored U_L31 and U_L34 genes. Cells were fixed in methanol and stained with purified egg immunoglobulin Y from chickens immunized with a human lamin A-GST fusion protein and a mouse monoclonal antibody against ICP4.

The data presented thus far do not distinguish between the possibilities that U_L34 mediates (i) a partial lamina dissolution or (ii) conformational changes that change the reactivity of lamin A/C to the rabbit polyclonal antibody. To attempt to distinguish between these possibilities, a chicken polyclonal immunoglobulin Y anti-lamin A/C antibody was generated as detailed in Materials and Methods. Cells were mock infected or infected with HSV-1(F), the U_L31 and U_L34 deletion viruses, or the U_L34 restored virus. The cells were then fixed and stained with the chicken antilamin antibody.

Like the commercial monoclonal antibody, the chicken anti-lamin A/C antibody stained the nuclear rim of mock-infected cells. Unlike the commercial rabbit polyclonal antibody, virtually no nucleoplasmic staining was observed. Importantly, the staining intensity of lamin A/C was similar regardless of whether the cells were infected or mock infected (Fig. 3). Taken together, the data indicate that while U_L34 is required for HSV-mediated alteration of the conformation of the nuclear lamina, this does not necessarily reflect a gross loss of lamin epitopes from the nuclear rim.

Lamin solubility in cells infected with wild-type HSV-1. Previous results indicated that, in HSV-infected cells, the solubility of lamins was dramatically increased over that in uninfected cells when extracted with 2 M NaCl (27). The observation that lamin A/C remained associated with the nuclear rim in in-

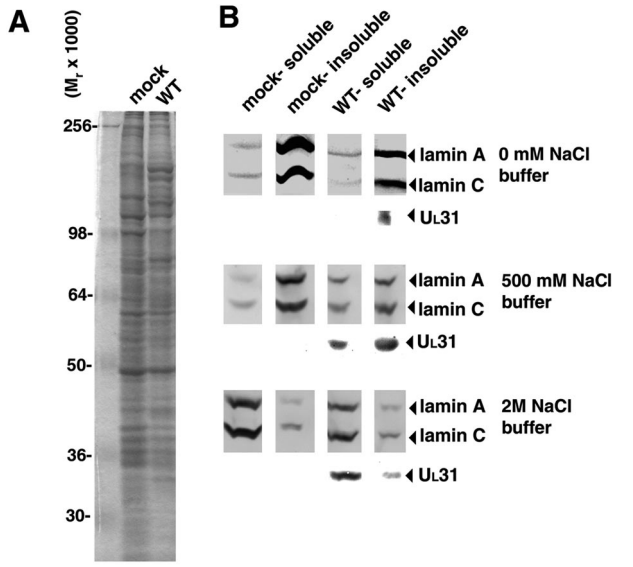

FIG. 4. (A) Electrophoretic profiles of infected and uninfected stained with Coomassie blue. HEp-2 cells were either mock infected or infected at an MOI of 5.0, and equal amounts of total protein, as determined by a modified Bradford assay, were resolved electrophoretically on an SDS-polyacrylamide gel and stained with Coomassie blue. Amounts of protein equivalent to that in each lane were extracted in the experiments shown in panel B. (B) Equal amounts of total protein from mock- and wild-type-infected lysates were harvested at 16 h postinfection and extracted with buffers containing 0 mM NaCl, 500 mM NaCl, or 2 M NaCl as described in Materials and Methods. Denatured soluble and insoluble fractions from the various buffer treatments were separated on an SDS–8% polyacrylamide gel and transferred to nitrocellulose, and the membrane was probed with lamin A/C antiserum. Bound anti-lamin antibody was detected with goat anti-mouse alkaline phosphatase-conjugated secondary antibody, followed by incubation with ECF substrate. The membrane was then scanned with a Molecular Dynamics Storm 860 PhosphorImager. Total counts were quantified with ImageQuant software. To determine the relative fractionation of U_L31 proteins in these extractions, the membrane was blocked overnight with 5% nonfat dry milk in sterile PBS and then reprobed with U_L31 protein-specific antiserum. U_L31 protein was detected with goat anti-rabbit alkaline phosphatase-conjugated antiserum and chromogenic substrates. The displayed image was generated by scanning with a digital scanner.

fected cells, albeit in a different conformation, suggested that, rather than being completely solubilized, most lamin A/C remained associated with the lamina or lamin receptors. The following additional experiments were undertaken to determine whether lamins were completely or incompletely solubilized in HSV-infected cells.

To determine the fate of lamin A/C in infected cells under various extraction conditions, HEp-2 cells were either mock infected or infected with HSV-1(F) and harvested at 16 h postinfection. The cells were treated with salt and detergent buffers, and the total protein concentration in the lysates was determined with a modified Bradford assay. A Coomassie gel illustrating the electrophoretic profiles of equivalent levels of total proteins from mock-infected and HSV-1(F)-infected HEp-2 whole-cell lysates is shown in Fig. 4A. Cells were extracted with buffers containing either 0 mM NaCl, 500 mM NaCl, or 2 M NaCl as detailed in Materials and Methods.

After extraction on ice, soluble and insoluble fractions were separated by centrifugation, and the two fractions were placed in separate tubes. In the case of the 500 mM and 2 M NaCl extracts, it was necessary to briefly sonicate the lysates before centrifugation to clearly resolve the two layers. Proteins recovered from the soluble and insoluble fractions were denatured in SDS, electrophoretically separated on an 8% denaturing polyacrylamide gel, and then probed with the mouse lamin A/C monoclonal antibody, followed by development with ECF reagent (Amersham). Chemiluminescence was recorded with a Molecular Dynamics PhosphorImager. The nitrocellulose sheet was then blocked and reprobed with rabbit polyclonal antiserum directed against the U_L31 protein. Bound antibody was identified by incubation with an alkaline phosphatase-conjugated anti-rabbit immunoglobulin G, followed by addition of chromogenic substrate. After color development, the nitrocellulose membrane was scanned to create the digital image shown in Fig. 4. The data are summarized in Table 2.

TABLE 2. Soluble lamin A/C in infected and uninfected cells[a]

NaCl concn	Soluble lamin A/C in HSV-1(F)-infected HEp-2 cells (%)	Soluble lamin A/C in uninfected HEp-2 cells (%)
0 mM	20–23[b]	20–23
500 mM	40–46[b], (50–55)[c]	25–28
2.0 M	60–70[c]	60–70[c]

[a] Cells were infected or mock infected, and cell pellets were subjected to extraction under the indicated salt conditions. Extractions were performed in triplicate under the various conditions. Relative amounts of lamin A/C were determined by quantifying the chemiluminescence of immunoblots (Fig. 4) reacted with a lamin A/C-specific antibody on a PhosphorImager.
[b] Cells were not sonicated during extractions.
[c] Cells were sonicated briefly during extractions to facilitate separation of soluble and insoluble material.

The percentage of solubilized lamin A/C was determined in triplicate for cells treated with each salt extraction buffer, and representative results of the extraction experiments are shown in Fig. 4B. The levels of lamin solubility in both infected and uninfected cells extracted with the detergent and 0 mM NaCl were comparable and approximated 20 to 23% of total lamin A/C. In uninfected cells extracted with the buffer containing 500 mM NaCl, the level of solubility increased to 25 to 28% of total lamin A/C. The level of solubility remained in this range regardless of whether the lysates were sonicated. In infected cells extracted with 500 mM NaCl, however, sonication before centrifugation facilitated demarcation of the soluble and insoluble phases and slightly increased the amount of lamin A/C proteins extracted. Specifically, 40 to 46% of total lamin A/C was extracted when the lysates were not sonicated, whereas 50 to 55% of lamin A/C was localized in the soluble phase when the material was sonicated.

Sonication of the equilibrated cellular lysates was necessary to separate the soluble and insoluble phases of both infected and uninfected cells extracted with 2 M NaCl. In contrast to the results obtained upon extraction with 500 mM NaCl, the amounts of lamin extracted with 2 M NaCl did not differ significantly between uninfected cells and infected cells. In both cases, approximately 60 to 70% of the total lamins were recovered in the supernatant. We conclude from this set of experiments that a relative increase in lamin A/C solubility in HSV-1(F)-infected HEp-2 cells compared to mock-infected

cells is detectable upon extraction at 500 mM NaCl but not upon extraction with 0 or 2 M NaCl.

When the blots were reprobed for U_L31 protein, it was observed that U_L31 protein solubility correlated with the solubility of lamin A/C. This cofractionation is consistent with the previous observation that U_L31 associates with the nuclear matrix (3) and is consistent with the possibility that U_L31 protein interacts either directly or indirectly with lamin A/C in infected cells.

In numerous experiments conducted to determine if electrophoretic mobility shifts of lamin proteins occurred during infection, no changes in mobility were noted. These data corroborate the studies of Radsak and colleagues demonstrating that HSV-1 infection does not induce altered electrophoretic mobilities of lamins in human fibroblast cells infected with wild-type HSV-1 (22, 23).

Transient overexpression of U_L31 protein is sufficient to disrupt the nuclear lamina and relocalize lamin A/C into the nucleoplasm. Normally, lamin A/C molecules are translated in the cytoplasm, imported into a soluble nuclear pool, and subsequently incorporated into the nuclear lamina. To determine the effects of U_L31 on localization of lamin A/C in the absence of other proteins, the U_L31 open reading frame was cloned into the vector pcDNA3.0 so that expression was driven by the human cytomegalovirus immediate-early promoter. HEp-2 cells were transfected with the expression plasmid and fixed with ice-cold methanol at 45 h postinfection at −20°C. Fixed cells were subsequently stained with lamin A/C-specific monoclonal antibody and rabbit polyclonal antiserum directed against the U_L31 protein. The results are shown in Fig. 5.

HEp-2 cells transiently overexpressing U_L31 protein were morphologically distinct from untransfected cells and cells transfected with vector plasmid pcDNA3 alone (not shown). In cells containing overexpressed U_L31 protein, lamin A/C accumulated in globular nucleoplasmic aggregates rather than mostly at the nuclear rim. Costaining for the U_L31 gene product revealed that lamin A/C and U_L31 protein colocalized within the nucleoplasmic aggregates. Similar lamin A/C displacement was noted in Vero cells transfected with the U_L31 expression construct (data not shown). When the transfected cells were examined by Nomarski microscopy, the nuclei of transfected cells clearly contained intranuclear aggregates, whereas other structures of the cell, including the nuclear membrane, remained largely unaltered. To confirm that this dramatic disruption of the lamina structure was not a consequence of apoptosis, monolayers of transfected cells were stained with propidium iodide and Hoechst stain. Propidium iodide uptake was not observed, and the Hoechst staining pattern was normal, with no apoptotic bodies detected (data not shown). These data indicate that overexpression of U_L31 in the absence of other HSV proteins is sufficient to displace the nuclear lamina from the nuclear rim.

Transient overexpression of the U_L34 protein is sufficient to relocalize some lamin A/C into the cytoplasm of some cells. HEp-2 cells transfected with a U_L34 expression plasmid were fixed in methanol 24 and 48 h after transfection, and the cells were stained for U_L34 protein and lamin A/C. Representative results at 24 h are shown in Fig. 5 and summarized in Table 3. Qualitatively similar results were obtained at 48 h posttransfection except that fewer cells were available for analysis (not shown). As shown previously (24), U_L34 protein accumulated in a perinuclear and cytoplasmic reticular pattern reminiscent of the endoplasmic reticulum when expressed in the absence of U_L31. Approximately 82% of cells containing detectable U_L34 protein contained at least some lamin A/C within the cytoplasm. The cytoplasmic lamin A/C did not colocalize extensively with cytoplasmic U_L34 protein. In contrast, only 1.6% of cells that did not contain detectable U_L34 protein contained detectable cytoplasmic lamin A/C. We conclude that transient expression of U_L34 protein can mediate the relocalization of some lamin A/C into the cytoplasm.

Coexpression of U_L31 and U_L34 and effects on lamin A/C distribution. To determine if the U_L31/U_L34 protein complex was sufficient to modify the nuclear lamina when coexpressed, HEp-2 cells were cotransfected with equal amounts of the U_L31 and U_L34 expression plasmids, fixed 24 h after transfection, and stained for U_L31, U_L34, and lamin A/C. The results indicated that, as noted previously, coexpression of U_L31 and U_L34 proteins causes the two proteins to colocalize at the nuclear rim. Lamin A/C was also located at the nuclear rim and to a lesser extent in the nucleoplasm of cells containing both U_L31 and U_L34 proteins. In many cells coexpressing the U_L31 and U_L34 proteins, the distribution of lamin A/C appeared more punctate than in cells not containing these proteins, but overall lamin staining was not markedly decreased, even in areas of the nuclear membrane where abundant U_L31 and U_L34 proteins were present. (Compare the two cells, one transfected and one not transfected, in Fig. 5C). Similar results were seen at 48 h after transfection (data not shown). We conclude that, at least under the conditions tested, the U_L31 and U_L34 proteins are insufficient to mimic the dramatically decreased lamin A/C staining seen in cells infected with wild-type HSV-1(F), suggesting that proteins other than those encoded by U_L31 and U_L34 are also required.

U_L31 and U_L34 proteins can interact directly with lamin A in vitro. To investigate whether lamin A physically interacts with the $U_L31$and U_L34 proteins in vitro, radiolabeled lamin A expressed in a rabbit reticulocyte lysate was incubated with equivalent amounts of GST or the U_L31-GST or U_L34-GST fusion protein bound to Sepharose beads. The beads were washed extensively, and associated proteins were eluted in SDS and electrophoretically separated on a denaturing polyacrylamide gel. Analysis with a PhosphorImager indicated that the level of lamin A was approximately 20-fold higher in lanes containing radiolabeled lamin A mixed with U_L31-GST than reaction mixtures containing GST alone. In the reciprocal reaction, radiolabeled U_L31 protein expressed in a rabbit reticulocyte lysate was incubated with 20 μg of GST or full-length lamin A-GST fusion protein. The amount of U_L31 protein associated with lamin A-GST was at least 50-fold higher than the level of U_L31 protein bound to GST alone (Fig. 6A). From these data, we conclude that U_L31 protein and lamin A interact physically in the context of a rabbit reticulocyte lysate.

A similar experiment was performed with radiolabeled U_L34 protein mixed with lamin A-GST and U_L34-GST mixed with radiolabeled lamin A. In this experiment (Fig. 6B), lamin A-GST pulled down at least 20-fold more U_L34 protein than did GST alone, and U_L34-GST pulled down at least 20-fold more lamin A than did GST alone. We therefore conclude that U_L34

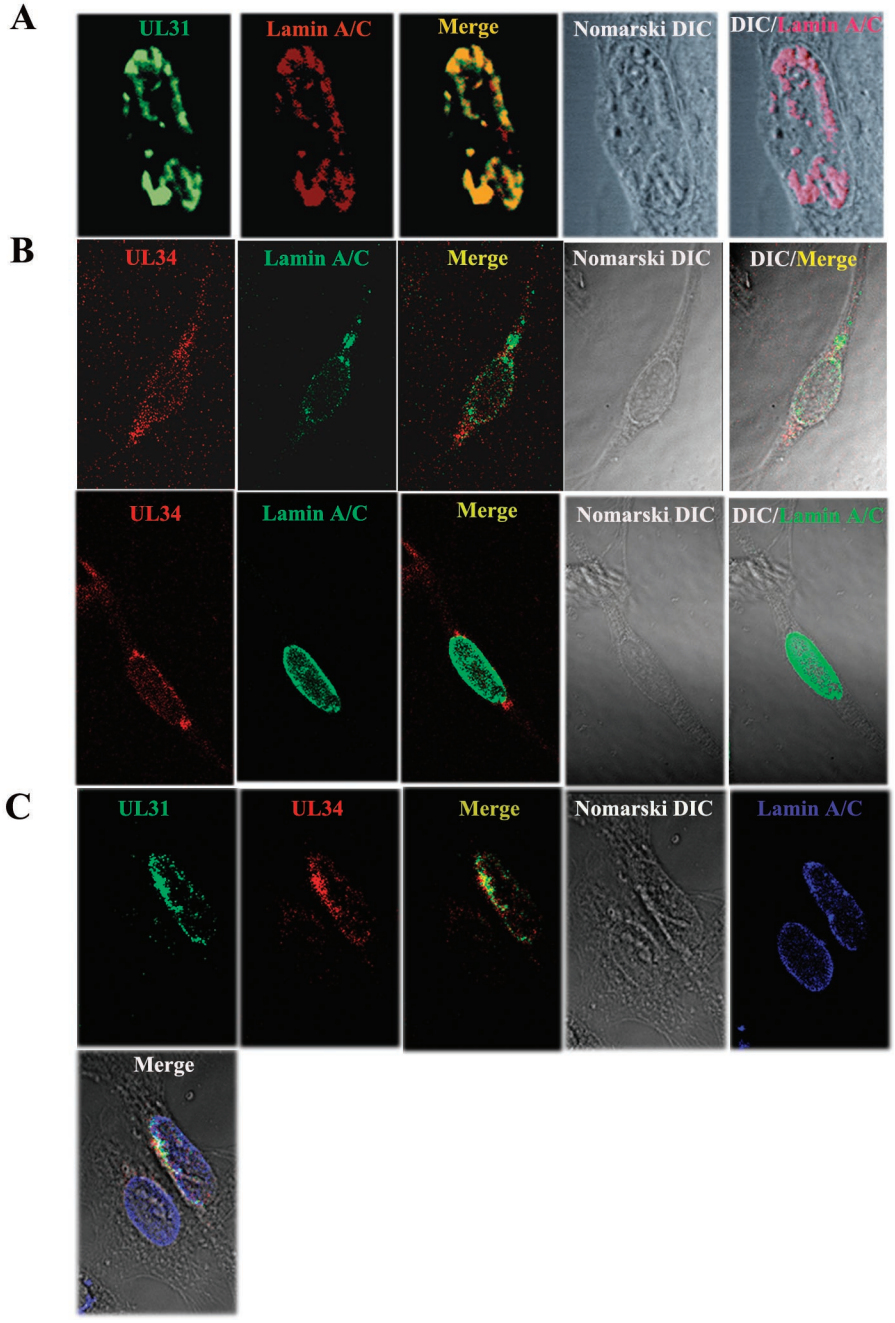

FIG. 5. (A) HEp-2 cells were transiently transfected with 4.5 μg of pJB233, a full-length U_L31/pcDNA3 construct. Cells were fixed and permeabilized at 45 h posttransfection and incubated with U_L31/GST-specific rabbit polyclonal antisera and lamin A/C monoclonal antibody. Bound antibodies were detected with Alexa 488 fluorophore-conjugated donkey anti-rabbit antibodies (green, U_L31 protein) and Alexa 568 fluorophore-conjugated donkey anti-mouse antibodies (red, lamins A/C). Areas of colocalization of the proteins are indicated by a yellow signal in the merged image. The differential interference contrast (DIC) image shown is of the same transfected cell. Images were acquired with a 63× oil objective. (B) HEp-2 cells were transiently transfected with 4.5 μg of pJB234, a full-length U_L34/pcDNA3 construct. Transfected cells were fixed and blocked with 10% BlockHen II (Aves Labs) and reacted with anti-U_L34 chicken antibody (1:4,000) and lamin A/C monoclonal antibody. Bound antibodies were detected with Texas Red-conjugated donkey anti-chicken immunoglobulin and FITC-conjugated donkey anti-mouse immunoglobulin. Two different images of the cells are shown: the upper panel shows a cell scored as having cytoplasmic lamin A/C, whereas the lower panel shows a cell having nuclear lamin A/C. Cumulative results are presented in Table 3. (C) HEp-2 cells were cotransfected with 2.5 μg of pJB233 together with 2.5 μg of pJB234. At 45 h posttransfection, cells were fixed in ice-cold methanol for 20 min at −20°C and rinsed thoroughly in PBS. The fixed cells were blocked with human serum and incubated with U_L31 protein-specific rabbit polyclonal antiserum, UL34 protein-specific chicken antiserum, and mouse anti-lamin A/C monoclonal antibody. Bound primary antibodies were detected with donkey anti-rabbit immunoglobulin conjugated with Alexa 488 fluorophore, donkey anti-chicken immunoglobulin conjugated with Alexa 568 fluorophore, and donkey anti-mouse immunoglobulin conjugated with indodicarbocyanine. Fluorescence and Nomarski differential interference contrast digital micrographs were collected with Fluoview software with a 63× oil objective. The lamin A/C-specific signal was pseudocolored blue for illustrative purposes.

TABLE 3. Effects of transient expression of U_L34 on localization of lamin A/C[a]

Cells	Cytoplasmic lamin staining [no. (%) of cells]		Total no. of cells counted
	Present	Absent	
Untransfected	4 (1.6)	245 (98.4)	249
Transfected	99 (82.5)	21 (17.5)	120

[a] Cells were transfected with a plasmid expressing U_L34 or left untransfected and stained for lamin A/C and U_L34 protein. Cells expressing and not expressing U_L34 were selected randomly, and whether lamin A/C-specific immunofluorescence was detected in the cytoplasm was noted.

can also interact with lamin A in the context of a rabbit reticulocyte lysate.

Mapping of sites within lamin A that interact with U_L31 protein. Based on the distribution of lamin A/C in infected cells stained with monoclonal antibody versus the appearance obtained with polyclonal antibodies, we hypothesized that some lamin A/C epitopes were partially masked in HSV-infected cells. Under the reasoning that the masked lamin A/C epitope would be located near the domain responsible for interaction with the U_L31/U_L34 protein complex, the relevant epitopes were mapped as follows. Small, overlapping domains (illustrated in Fig. 7A) of lamin A were amplified by PCR and cloned in frame with the gene encoding GST. Equal amounts of the resulting GST fusion proteins were electrophoretically resolved by SDS-PAGE and transferred to nitrocellulose. The nitrocellulose sheet was then reacted separately with the rabbit polyclonal and mouse monoclonal antibodies directed against lamin A/C. The results of this experiment, shown in Fig. 7B to D, definitively indicated that the lamin A/C-specific monoclonal antibody bound to lamin A residues contained in the GST/Tail 1 fusion protein (lamin A amino acids 369 to 519), whereas the rabbit polyclonal antibody recognized the GST/Rod1 fusion protein (containing lamin A amino acids 117 to 239) and to a lesser extent the GST/Rod2 fusion protein (containing lamin A amino acids 216 to 384).

The dramatic rearrangement of the nuclear lamina induced by overexpression of U_L31 protein was reminiscent of the appearance of cells containing overexpressed truncated lamins (15). In these cases, the truncated lamins competed for and disrupted lamin-lamin or lamin-lamin receptor interactions, causing lamins to relocalize in the nucleoplasm. To determine if U_L31 mediated lamin rearrangement in a similar fashion, we conducted a series of experiments to more directly map the sites of lamin A that interacted with U_L31 protein. The series of lamin A-GST fusion proteins were therefore tested for their ability to pull down full-length U_L31 protein expressed in rabbit reticulocyte lysates. As shown in Fig. 7E, both lamin tail 1 and tail 2 pulled down in vitro-expressed U_L31 protein, whereas other lamin domains did not interact substantially above the level with GST alone. From these data, we conclude that U_L31 protein either binds to unique regions of tail 1 and tail 2 or binds the overlapping region of these two domains. Because these regions are not known to be directly involved in lamin-lamin interactions or lamin-lamin receptor interactions (such functions are ascribed to rod domains or rod junction domains), we conclude that the mechanism by which U_L31 protein facilitates lamina rearrangements is not necessarily the same as that mediated by overexpression of truncated lamins.

DISCUSSION

This study shows that HSV-1 infection modifies the nuclear lamina, masking several different epitopes within the tail and rod domains of lamin A/C. We also found that the U_L31 and U_L34 proteins are necessary for masking of the epitope located

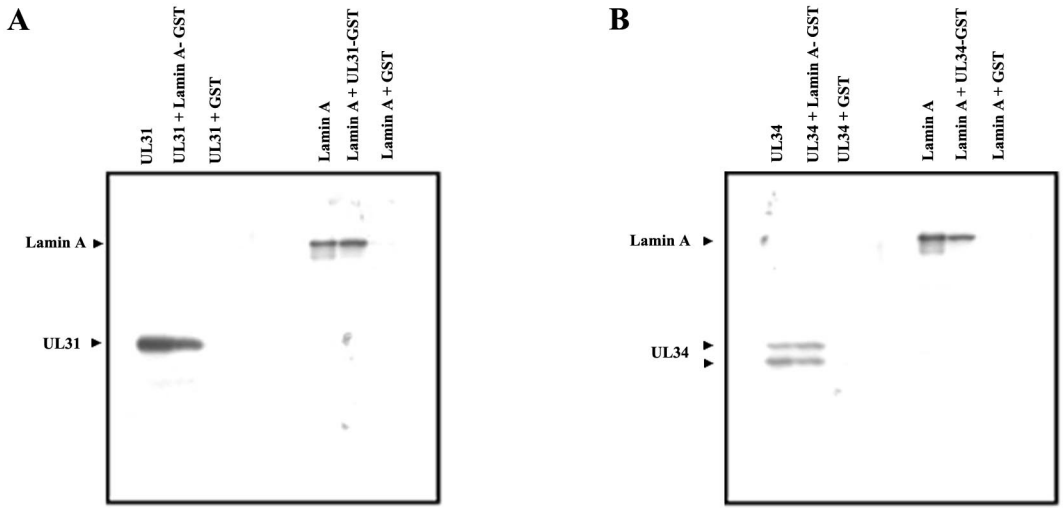

FIG. 6. (A) Scanned digital image of GST pulldown reactions. Full-length U_L31 protein and lamin A were expressed and radiolabeled with [35S]methionine in a rabbit reticulocyte lysate. The radiolabeled proteins are indicated to the left. Radiolabeled U_L31 protein was reacted with lamin-GST fusion protein or GST alone bound to glutathione-Sepharose beads (left lanes), and radiolabeled lamin A was reacted with U_L31-GST or GST alone bound to glutathione-Sepharose beads (right lanes). After extensive washing of the beads with cold PBS supplemented with 1% Triton X-100, associated proteins were eluted, denatured, and electrophoretically separated on a 10% polyacrylamide gel. The gel was impregnated with sodium salicylate, dried, and fluorographed. The developed radiographic film was then digitally scanned. (B) Experiments were performed as in panel A except that GST-U_L34 was reacted with radiolabeled lamin A and radiolabeled U_L34 protein was reacted with lamin A-GST.

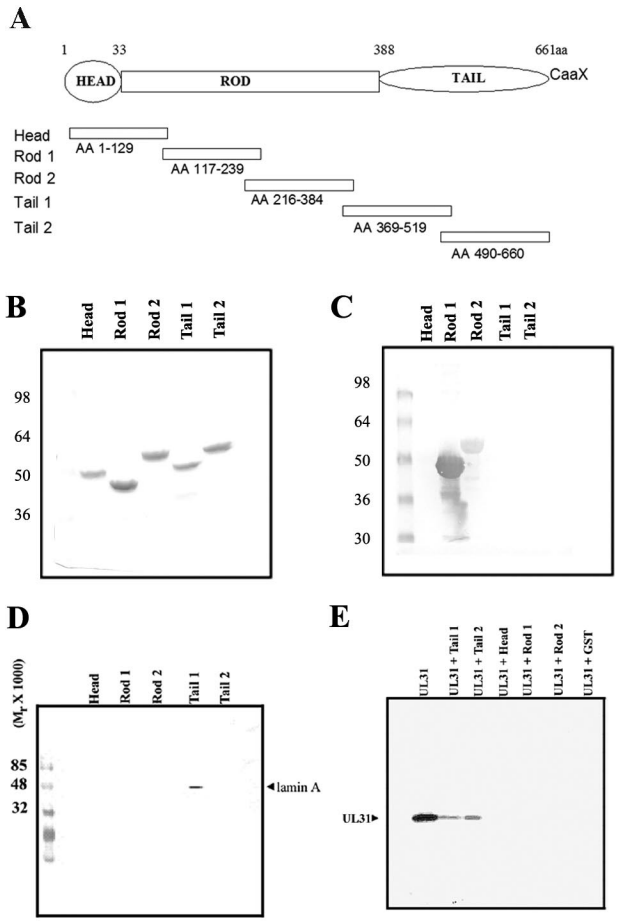

FIG. 7. (A) Schematic drawing illustrating the amino acids contained within the lamin subdomains designated GST/Head, GST/Rod1, GST/Rod2, GST/Tail1, and GST/Tail2. The regions encoding these domains were PCR amplified with the primers shown in Table 1. These domains were cloned into pGEX2T for expression and purification. (B) Digital image of purified lamin-GST fusion proteins diagrammed in panel A. Purified proteins were electrophoretically separated on a denaturing gel and stained with Coomassie blue. Protein designations are indicated above the figure. (C) Scanned digital image of an immunoblot of the indicated lamin-GST fusion proteins probed with rabbit polyclonal anti-lamin A/C antibody. (D) Scanned digital images of GST fusion proteins with lamin head, rod 1, rod 2, tail 1, and tail 2 electrophoretically resolved, transferred to nitrocellulose, and probed with the commercial lamin A/C monoclonal antibody. (E) Fluorographic images of lamin-GST pulldowns reacted with full-length U_L31 protein. ^{35}S-labeled U_L31 protein was expressed in a rabbit reticulocyte lysate and reacted in cold PBS supplemented with 1% Triton X-100 with equal amounts of GST or one of several GST fusion proteins bearing regions of lamin A bound to glutathione Sepharose beads. After extensive washing with the Triton X-100 buffer, the protein mixture was resolved on a 10% acrylamide gel, and fluorographic images were obtained as described in the legend to Fig. 6.

in the tail domain and that U_L34 is required for the HSV-mediated masking of epitopes within the rod domain even in the absence of U_L31.

We have also shown that overexpression of U_L31 protein can mediate lamin A/C displacement from the nuclear rim into nucleoplasmic aggregates, whereas overexpression of U_L34 can mediate limited displacement of lamin A/C into the cytoplasm. The location of displaced lamins reflects the localization of each HSV protein when overexpressed in the absence of the other. Thus, U_L31 protein localizes in the nucleoplasm, whereas U_L34 redistributes partly to the nuclear rim but also to the cytoplasm (24). The appearance of lamin A/C distribution and lamina disruption induced upon U_L31 overexpression is reminiscent of overexpression of dominant negative lamin A/C lacking either the head or tail domain (15). It is currently unclear whether this observation reflects a role for U_L31 in localized lamina disruption in HSV-infected cells or simply reflects the fact that the protein binds lamin A/C and, when overexpressed, competes destructively for lamin-lamin or lamin-lamin receptor interactions. Because the tail regions of lamin A/C shown to be sufficient to bind U_L31 protein are not those that normally mediate lamin-lamin interactions, it seems more likely that U_L31 protein acts to disrupt the lamina indirectly rather than through a strict competition between U_L31 and lamin-lamin interactions. On the other hand, U_L34 protein does decrease the reactivity of lamin rod epitopes in HSV-infected cells, and such domains likely mediate lamin-lamin interactions. Although U_L34 protein can interact with lamin A/C in vitro, preliminary evidence does not indicate that U_L34 interacts with lamin A/C rod domains directly (not shown). Thus, it is likely that U_L34 may serve to alter lamin A/C rod domain epitopes indirectly.

Consistent with this conclusion is the observation that when U_L31 and U_L34 proteins are coexpressed, the two proteins colocalize at the nuclear rim, and in these cells, lamin A/C is not dramatically displaced from the nuclear rim, nor is lamin A/C staining decreased. Other HSV-encoded proteins that accumulate at the inner nuclear membrane would be logical candidates to contribute to the alteration of lamin epitopes. Such proteins include glycoproteins B and D and the product of U_L11 (2, 31).

Just as U_L31 and U_L34 are coexpressed in the absence of other HSV proteins, gross mislocalization of lamin A/C to areas other than the nuclear rim does not occur in the context of a viral infection (Fig. 5). It is logical to propose that coexpression limits the diffusion of the U_L31/U_L34 protein complex to the nuclear membrane, precluding obvious lamin A/C displacement to regions other than the nuclear rim. Limiting any potential destructive effects on the lamina would be expected to preserve functions of the nucleus that are necessary for viral replication. At the same time, localization of U_L31 and U_L34 in specific regions of the nuclear membrane might concentrate any capacity of the complex to conformationally alter the lamina in localized regions.

Taken together, the current data suggest that the lamina is only locally disrupted or perhaps thinned, a possibility that was originally suggested by Scott and O'Hare (27). Data supporting this conclusion is the observation that only limited differences in the amount of total extractable lamin A/C were noted between mock-infected cells and those infected with wild-type virus. Thus, whereas 25% of lamins A and C were extracted from uninfected cells at 500 mM NaCl, 40 to 55% of total lamins were extracted from infected cells, depending on whether sonication was performed during extraction. In contrast, no significant differences in lamin A/C solubility were observed in uninfected versus. infected cells that were extracted with 0 or 2 M NaCl. It is also noteworthy that we did not identify experimental conditions resulting in 100% solubi-

lization of lamin protein, in contrast to the findings of others (27).

Potential differences between the previous study and the current one include the following. First, whereas the previous study used COS-1 cells for their assays, HEp-2 cells were used in the current study. However, we performed similar experiments with COS-1 cells and obtained results comparable to those reported upon extraction of HEp-2 cells (data not shown). Second, the previous study discussed equilibration of total cellular protein based on the appearance of the electrophoretic profiles as revealed by Coomassie blue staining of SDS-polyacrylamide gels. In the current study, the total protein concentrations of the cellular lysates were equilibrated before extraction with a modified Bradford assay. Finally, given the variability of the amounts of lamins extracted under various salt conditions, variations in extraction technique might alter the results obtained.

It has been proposed that MCMV recruits isoforms of protein kinase C to the nuclear lamina and exploits this as a mechanism to dissociate lamins from the inner nuclear membrane (20). In the absence of any obvious electrophoretic differences in lamins A and C from infected and uninfected cells as found in this study and as described previously (23), we propose different mechanisms to explain how the HSV-1 U_L31 and U_L34 proteins might facilitate the egress of nucleocapsids.

Our favored hypothesis is that the U_L31- and U_L34-mediated alteration of lamin A/C reflects a local thinning or conformational modification that promotes access of nucleocapsids to the inner nuclear membrane. The data suggest that this is a consequence of direct or indirect interaction of these proteins with lamin A/C in the nuclear lamina. Although the data indicate that HSV induces conformational changes in lamin A/C, models proposing roles for the U_L31 and U_L34 proteins in the egress of nucleocapsids must also account for the fact that in infected cells stained with at least one lamin A/C-specific antibody, the intensity and overall distribution of lamin A/C are similar in infected and uninfected cells. Given the fact that HSV capsids are only 120 nm in diameter, however, light microscopy might easily overlook effective permeabilization or localized thinning of the lamina that would allow capsids access to the nuclear membrane. More thorough investigation of this question by immunoelectron microscopy seems warranted.

It is also possible that interaction of U_L31 protein with the lamin tail domain competes with lamin A/C for interaction with chromatin. Less chromatin in regions of the nucleus could conceivably enhance exposure of the nucleoplasmic face of the inner nuclear membrane and thereby facilitate the egress of nucleocapsids. Since amino acids 411 to 553 of lamin A/C comprise a globular DNA binding domain that helps mediate association with chromatin (5, 13, 17, 28, 30), it was of interest that, through epitope mapping and GST pulldown reactions, we have determined that amino acids in or near the lamin A tail domain (amino acids 369 to 519 and 490 to 660) are sufficient to interact with U_L31 protein.

A third, nonexclusive possibility is that the U_L31 and U_L34 proteins may simply exploit binding to lamin A/C as a means to target the proteins to the nuclear lamina and nuclear membrane. Interaction with lamin A/C would potentially facilitate the interaction of the U_L34 and U_L31 proteins as they become concentrated at the nuclear membrane in regions containing lamin A/C. Once properly localized, the complex could then serve other functions that promote nucleocapsid envelopment, such as recruitment of other proteins to specific sites in the nuclear membrane or facilitating budding by interacting with nucleocapsids.

ACKNOWLEDGMENTS

We are grateful to David Gilbert (Upstate Medical Center, SUNY Syracuse) for providing the wild-type and mutant lamin A constructs, Willliam Ruyechan for the ICP8 antiserum, and Richard Roller for the U_L34 deletion virus and U_L34 repair virus and U_L34 antiserum. We thank Karin Darpel for assistance in the initial cloning of the lamin constructs and acknowledge the technical excellence of Elizabeth Wills and Jarek Okulicz-Kozaryn. We acknowledge all the members of the Baines laboratory for helpful discussions in support of this work. We also thank the reviewers for the suggestion to investigate the effect of U_L34 protein on the nuclear lamina.

These studies were supported by NIH R01 grants GM50740 and AI52341 to J.D.B. and National Research Service Award F32 GM20448 to A.E.R.

REFERENCES

1. **Baines, J. D., A. H. Koyama, T. Huang, and B. Roizman.** 1994. The U_L21 gene of herpes simplex virus 1 is dispensable for replication in cell culture. J. Virol. **68:**2929–2936.
2. **Baines, J. D., R. J. Jacob, L. Simmerman, and B. Roizman.** 1995. The U_L11 gene products of herpes simplex virus 1 are present in the nuclear and cytoplasmic membranes and intranuclear dense bodies of infected cells. J. Virol. **69:**825–833.
3. **Chang, Y. E., and B. Roizman.** 1993. The product of the U_L31 gene of herpes simplex virus 1 is a nuclear phosphoprotein which partitions with the nuclear matrix. J. Virol. **67:**6348–6356.
4. **Chang, Y. E., C. Van Sant, P. W. Krug, A. E. Sears, and B. Roizman.** 1997. The null mutant of the U_L31 gene of herpes simplex virus 1: construction and phenotype of infected cells. J. Virol. **71:**8307–8315.
5. **Dhe-Paganon, S., E. D. Werner, Y. I. Chi, and S. E. Shoelson.** 2002. Structure of the globular tail of nuclear lamin. J. Biol. Chem. **277:**17381–17384.
6. **Ejercito, P. M., E. D. Kieff, and B. Roizman.** 1968. Characterization of herpes simplex virus strains differing in their effects on social behavior of infected cells. J. Gen. Virol. **2:**357–364.
7. **Fisher, D. Z., N. Chaudhary, and G. Blobel.** 1986. cDNA sequencing of nuclear lamins A and C reveals primary and secondary structural homology to intermediate filament proteins. Proc. Natl. Acad. Sci. USA **83:**6450–6454.
8. **Frangioni, J. V., and B. G. Neel.** 1993. Solubilization and purification of enzymatically active glutathione-S-transferase (pGEX) fusion proteins. Anal. Biochem. **210:**179–187.
9. **Fuchs, W., B. G. Klupp, H. Granzow, N. Osterrieder, and T. C. Mettenleiter.** 2002. The interacting UL31 and UL34 gene products of pseudorabies virus are involved in egress from the host-cell nucleus and represent components of primary enveloped but not mature virions. J. Virol. **76:**364–378.
10. **Gant, T. M., and K. L. Wilson.** 2000. Nuclear assembly. Annu. Rev. Cell Dev. Biol. **13:**669–695.
11. **Gruenbaum, Y., K. L. Wilson, A. Harel, M. Goldberg, and M. Cohen.** 2000. Review: nuclear lamins—structural proteins with fundamental functions. J. Struct. Biol. **129:**313–323.
12. **Hoger, T. H., G. Krohne, and W. W. Franke.** 1988. Amino acid sequence and molecular characterization of murine lamin B as deduced from cDNA clones. Eur. J. Cell Biol. **47:**283–290.
13. **Hoger, T. H., G. Krohne, and J. A. Kleinschmidt.** 1991. Interaction of Xenopus lamins A and LII with chromatin in vitro mediated by a sequence element in the carboxyterminal domain. Exp. Cell Res. **197:**280–289.
14. **Hoger, T. H., K. Zatloukal, I. Waizenegger, and G. Krohne.** 1990. Characterization of a second highly conserved B-type lamin present in cells previously thought to contain only a single B-type lamin. Chromosoma **100:**67–69.
15. **Izumi, M., O. A. Vaughan, C. J. Hutchison, and D. M. Gilbert.** 2000. Head and/or CaaX domain deletions of lamin proteins disrupt preformed lamin A and C but not lamin B structure in mammalian cells. Mol. Biol. Cell **11:**4323–4337.
16. **Knipe, D. M., D. Senechek, S. A. Rice, and J. L. Smith.** 1987. Stages in the nuclear association of the herpes simplex virus transcriptional activator protein ICP4. J. Virol. **61:**276–284.
17. **Krimm, I., C. Ostlund, B. Gilquin, J. Couprie, P. Hossenlopp, J. P. Mornon, G. Bonne, J. C. Courvalin, H. J. Worman, and S. Zinn-Justin.** 2002. The Ig-like structure of the C-terminal domain of lamin A/C, mutated in muscular dystrophies, cardiomyopathy, and partial lipodystrophy. Structure (Cambridge) **10:**811–823.

18. **Lin, F., and H. J. Worman.** 1993. Structural organization of the human gene encoding nuclear lamin A and nuclear lamin C. J. Biol. Chem. **268:**16321–16326.
19. **McKeon, F. D., M. W. Kirschner, and D. Caput.** 1986. Homologies in both primary and secondary structure between nuclear envelope and intermediate filament proteins. Nature **319:**463–468.
20. **Muranyi, W., J. Haas, M. Wagner, G. Krohne, and U. H. Koszinowski.** 2002. Cytomegalovirus recruitment of cellular kinases to dissolve the nuclear lamina. Science **297:**854–857.
21. **Osterrieder, A. Neubauer, C. Brandmuller, O. R. Kaaden, and D. J. O'Callaghan.** 1998. The equine herpesvirus 1 IR6 protein that colocalizes with nuclear lamins is involved in nucleocapsid egress and migrates from cell to cell independently of virus infection. J. Virol. **72:**9806–9817.
22. **Radsak, K., D. Schneider, E. Jost, and K. H. Brucher.** 1989. Alteration of nuclear lamina protein in human fibroblasts infected with cytomegalovirus (HCMV). Arch. Virol. **105:**103–112.
23. **Radsak, K. D., K. H. Brucher, and S. D. Georgatos.** 1991. Focal nuclear envelope lesions and specific nuclear lamin A/C dephosphoylation during infection with human cytomegalovirus. Eur. J. Cell Biol. **54:**299–304.
24. **Reynolds, A. E., B. Ryckman, J. D. Baines, Y. Zhou, L. Liang, and R. J. Roller.** 2001. U_L31 and U_L34 proteins of herpes simplex virus type 1 form a complex that accumulates at the nuclear rim and is required for envelopment of nucleocapsids. J. Virol. **75:**8803–8817.
25. **Reynolds, A. E., E. G. Wills, R. J. Roller, B. J. Ryckman, and J. D. Baines.** 2002. Ultrastructural localization of the HSV-1 U_L31, U_L34, and U_S3 proteins suggests specific roles in primary envelopment and egress of nucleocapsids. J. Virol. **76:**8939–8952.
26. **Roller, R., Y. Zhou, R. Schnetzer, J. Ferguson, and D. Desalvo.** 2000. Herpes simplex virus type 1 U_L34 gene product is required for viral envelopment. J. Virol. **74:**117–129.
27. **Scott, E. S., and P. O'Hare.** 2001. Fate of the inner nuclear membrane protein lamin b receptor and nuclear lamins in herpes simplex virus type 1 infection. J. Virol. **75:**8818–8830.
28. **Stierle, V., J. Couprie, C. Ostlund, I. Krimm, S. Zinn-Justin, P. Hossenlopp, H. J. Worman, J. C. Courvalin, and I. Duband-Goulet.** 2003. The carboxyl-terminal region common to lamins A and C contains a DNA binding domain. Biochemistry **42:**4819–4828.
29. **Stuurman, N., S. Heins, and U. Aebi.** 1998. Nuclear lamins: their structure, assembly, and interactions. J. Struct. Biol. **122:**42–66.
30. **Taniura, H., C. Glass, and L. Gerace.** 1995. A chromatin binding site in the tail domain of nuclear lamins that interacts with core histones. J. Cell Biol. **131:**33–44.
31. **Torrisi, M. R., C. Di Lazzaro, A. Pavan, L. Pereira, and G. Campadelli-Fiume.** 1992. Herpes simplex virus envelopment and maturation studies by fracture label. J. Virol. **66:**554–561.
32. **Yamauchi, Y., C. Shiba, F. Goshima, A. Nawa, T. Murata, and Y. Nishiyama.** 2001. Herpes simplex virus type 2 UL34 protein requires UL31 protein for its relocation to the internal nuclear membrane in transfected cells. J. Gen. Virol. **82:**1423–1428.
33. **Ye, G. J., and B. Roizman.** 2000. The essential protein encoded by the UL31 gene of herpes simplex virus 1 depends for its stability on the presence of the U_L34 protein. Proc. Natl. Acad. Sci. USA **97:**11002–11007.
34. **Ye, G. J., K. T. Vaughan, R. B. Vallee, and B. Roizman.** 2000. The herpes simplex virus 1 U_L34 protein interacts with a cytoplasmic dynein intermediate chain and targets nuclear membrane. J. Virol. **74:**1355–1363.
35. **Zhu, H. Y., H. Yamada, Y. M. Jiang, M. Yamada, and Y. Nishiyama.** 1999. Intracellular localization of the UL31 protein of herpes simplex virus type 2. Arch. Virol. **144:**1923–1935.